EPJ D
Atomic, Molecular, Optical and Plasma Physics
EPJ.org
your physics journal

Eur. Phys. J. D **65**, 563–570 (2011) DOI: 10.1140/epjd/e2011-20408-5

Resonant laser tunnelling

S. De Leo and P. Rotelli

EDP SCIENCES
Società Italiana di Fisica
Springer

Eur. Phys. J. D **65**, 563–570 (2011)
DOI: 10.1140/epjd/e2011-20408-5

THE EUROPEAN PHYSICAL JOURNAL D

Regular Article

Resonant laser tunnelling

S. De Leo[1,a] and P. Rotelli[2]

[1] Department of Applied Mathematics, State University of Campinas, P.O. Box 6065, 13083-970 Campinas, Brazil
[2] Department of Physics, University of Salento and INFN Lecce, Italy

Received 11 July 2011 / Received in final form 14 September 2011
Published online 1st December 2011 – © EDP Sciences, Società Italiana di Fisica, Springer-Verlag 2011

Abstract. We propose an experiment involving a gaussian laser tunneling through a twin barrier dielectric structure. Of particular interest are the conditions upon the incident angle for resonance to occur. We provide some numerical calculations for a particular choice of laser wave length and dielectric refractive index which confirm our expectations.

1 Introduction

In previous articles [1,2], we pointed out the analogies between laser interactions with a dielectric block and nonrelativistic quantum mechanics (NRQM). Tests of the latter physics should be easier through use of this optical analog, if only because we do not have to deal with probability amplitudes. One example is the transition in NRQM barrier diffusion from complete coherence to complete incoherence. Resonance phenomena occurs for the former limit but is absent in the latter. For example, the condition for coherence in *one-dimensional* NRQM diffusion is that the spatial size of the single incoming wave packet be much larger than the barrier size [3,4]. With coherence a single wave packet is transmitted. With complete incoherence, unlimited numbers of wave packets are transmitted at regular intervals. Whence, incoherence phenomena are absent when considering only a *single* incoming plane wave because of its infinite size. Within the laser/dielectric analogy the wave packet size is substituted by the laser beam transverse spreads. Interacting with a dielectric block, as expected from geometric optics, multiple reflections occur [5]. Coherence attains only if overlaps dominate in the outgoing laser spots. One important difference between optics and NRQM is that the optical situation is *stationary*. Time in NRQM is essentially replaced by a spatial variable in optics. This offers some significant advantages, e.g. even low intensity beams can be detected by long time exposures in detectors.

The fact that optical experiments provide an easy way to test quantum mechanical predictions, since the early 1970's, stimulated experimental and theoretical studies on quantum-optical analogies [6–14]. For clear and detailed reviews on the correspondence between optics and quantum mechanics, we refer the reader to the works of Dragoman [15] and Longhi [16].

[a] e-mail: deleo@ime.unicamp.br

Since any realistic setup is three dimensional, we must also work theoretically in three dimensions. Even when all interesting physics is dominantly bi-dimensional, e.g. the y-z plane defined by the incoming central laser direction (chosen by us as the z direction) and the normal to a structured dielectric system. There is a benefit in the extension beyond a simple one dimensional study to more dimensions. It means that the variation in "energy" in one-dimensional NRQM [17] can now be achieved by merely changing the incident angle. Indeed, it is the normal momentum component which now plays the role of energy in one dimension. For example, in optics, we can, under certain conditions, transit from diffusion to tunneling by simply rotating the dielectric structure relative to the incoming beam.

A dielectric-air-dielectric system mimics a potential barrier. Experiments realized by a double prism arrangement [18,19] have recently discussed the phenomenon of frustrated total internal reflection. In this paper, we go beyond a dielectric-air-dielectric system and consider a double prism plus a narrow slab separated by small air gaps of *equal size* (see Fig. 1). This reproduces a twin barrier situation [20–22] which should exhibit one of the most intriguing results of NRQM, the resonant tunneling effect [23,24]. Notwithstanding the expected attenuation of each barrier (air gap) upon the laser beam, for certain angular incidences the transition probability through twin barriers becomes unity, i.e. *total transmission* occurs. We determine the conditions for this phenomenon and reproduce sample results from a numerical calculation which necessarily takes into account the finite angular spread of any laser beam. By eliminating the intermediate slab, we reproduce the result of tunnelling through a single barrier [25,26]. The twin-barrier transmission results are attenuated by the entry/exit transmission amplitudes. All three must be folded into the laser momentum amplitude before integrating. This yields the outgoing laser beam amplitude and consequent intensity. For our analysis it

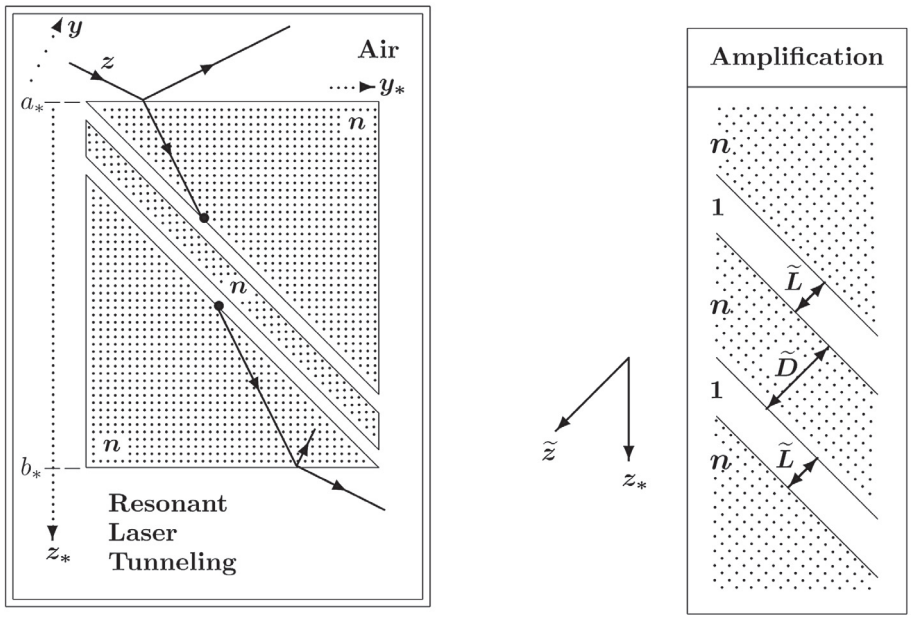

Fig. 1. Schematic presentation of a double prism plus a narrow slab separated by air gaps.

is advisable to avoid the complication of multiple outgoing beams produced by incoherences within the dielectric prisms. This is probably best achieved by considering only small incident angles α. In principle it could also be achieved by reducing the depth of the prisms. This would facilitate the search for resonance at larger incident angles. Another effect that would also help in the use of larger incident angles, without lose of coherence within the prisms, is the fact that the y-profile of the laser beam is increased with α as $1/\cos\alpha$. The x-profile is constant throughout and plays no role in the question of coherence. In the next section, we describe our theoretical treatment of the gaussian laser. In the subsequent section, we describe our proposed twin barriers structure. In Section 4, we provide the transmission/reflection probabilities for entry, exit and for the twin barriers. Section 5 contains our numerical transmission results for a chosen laser wave length and dielectric refractive index. The results confirm our phenomenological expectations. Our conclusions are drawn in the final section.

2 The Gaussian laser

Discussion of the laser is simplified by first concentrating upon the electric amplitude it produces and, wherever possible treating the amplitude as if it where a scalar. This amplitude is a convolution in wave number of plane waves. For different plane wave directions the polarization vector necessarily changes since it lies in the plane perpendicular to the wave direction $\boldsymbol{k}$. However, for a *sharp* gaussian in k_x and k_y we may assume to a good approximation that this vector (if linearly polarized) points in a fixed direction,

$$\boldsymbol{E}(x,y,z) = \{E_s(x,y,z), E_p(x,y,z)\},$$

where E_s is the component of the electric field perpendicular to the plane of incidence (s-polarization) and E_p is the component perpendicular to this plane (p-polarization).

In this paper, we shall present the discussion of resonant tunneling for a gaussian He-Ne laser, $\lambda = 633$ nm, of width $w_0(=2$ mm) which, in free space, propagates with principal axis along the z-direction, i.e.

$$G\left(k_x, k_y\right) = \exp\left[-\frac{w_0^2}{4}\left(k_x^{\,2} + k_y^{\,2}\right)\right]. \tag{1}$$

To simplify our presentation, we shall suppose that the laser beam passes through a linear polarizer which selects the s-polarization. This allows, as shown in the next section, to directly use the QM results. The electric field can be thus treated as a scalar,

$$\boldsymbol{E}(x,y,z) = \{E_s(x,y,z), E_p(x,y,z)\} = \{E(x,y,z), 0\},$$

where

$$E(x,y,z) = E_0\,\frac{\mathrm{w}_0^2}{4\,\pi}\int \mathrm{d}k_x\,\mathrm{d}k_y\; G\left(k_x,k_y\right) e^{i(k_x\,x + k_y\,y + k_z\,z)}. \tag{2}$$

Observing that $kw_0 = 2\pi w_0/\lambda \gg 1$, we find the following analytic analytic expression for the free space intensity,

$$\mathrm{I}(x,y,z) = \mathrm{I}_0\,\frac{w_0^2}{\mathrm{w}^2(z)}\,\exp\left[-2\frac{x^{\,2} + y^{\,2}}{\mathrm{w}^2(z)}\right],$$

$$\mathrm{w}(z) = w_0\sqrt{1 + \left(\frac{\lambda\; z}{\pi\, w_0^2}\right)^{2}}. \tag{3}$$

3 Layout of twin barrier apparatus

In Figure 2, we show the y-z overview of a prism which forms a part of a twin barrier structure. The incident ray

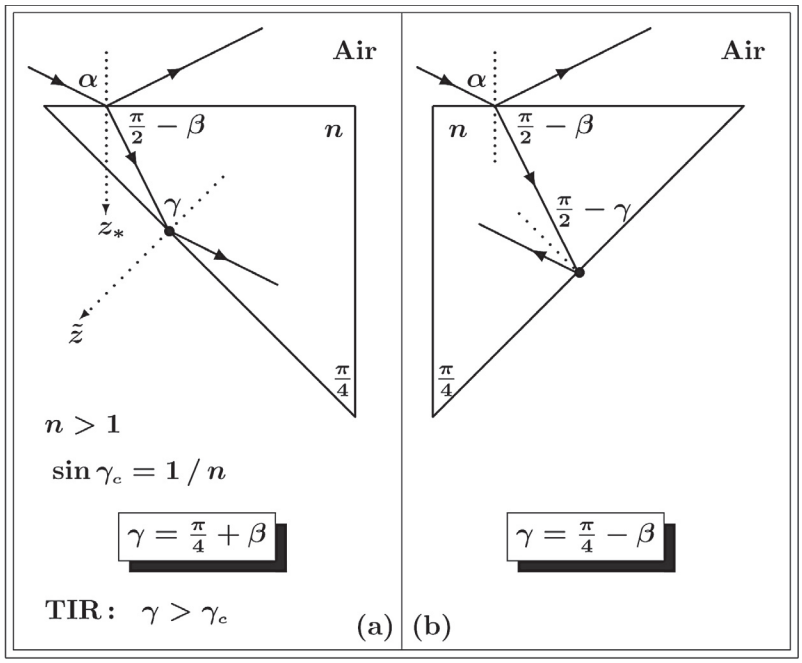

Fig. 2. Schematic presentation of a diagonally sliced dielectric prism. In the case (a), the condition $n > \sqrt{2}$ guarantees TIR for all the incidence angles ($0 \leq \sin\alpha \leq 1$). In the case (b), we have TIR for $n > \sqrt{2}$ and $0 \leq \sin\alpha \leq \sqrt{n^2 - 2\sqrt{n^2-1}}/\sqrt{2}$.

corresponding to the central direction of the laser travels along the z-axis. The incident angle with the normal, z_*, of the leading face of the dielectric is denoted by α. The internal direction β satisfies Snell's law,

$$\sin\alpha = n\,\sin\beta. \tag{4}$$

Before to derive the conditions for total internal reflection (TIR), let us establish the connection between optical and quantum mechanical problems. This connection will be the starting point for the calculation of the transmission probabilities presented in the next section.

The Fresnel formulas for the reflected and transmitted waves obtained when s-polarized light moves from air to a dielectric of a given refractive index n are [5]

$$R_s = \frac{\cos\alpha - n\cos\beta}{\cos\alpha + n\cos\beta} \quad \text{and} \quad T_s = \frac{2\,\cos\beta}{\cos\alpha + n\cos\beta}. \tag{5}$$

The air dielectric system is, for s-polarized incoming waves, the NRQM analog of a step potential. Indeed, for a step potential with a discontinuity perpendicular to the z_*-axis we obtain the following reflection and transmission coefficients [17]

$$R_{step} = \frac{k_{z_*} - q_{z_*}}{k_{z_*} - q_{z_*}} \quad \text{and} \quad T_{step} = \frac{2\,k_{z_*}}{k_{z_*} - q_{z_*}}. \tag{6}$$

Now, observing that for plane wave

$$k_{z_*} = k\cos\alpha \quad \text{and}$$
$$q_{z_*} = \sqrt{n^2k^2 - k_{y_*}} = \sqrt{n^2k^2 - k^2\sin^2\alpha} = n\,k\,\cos\beta,$$

we find $R_{step} = R_s$ and $T_{step} = T_s$. This analogy can be claimed even if there are subsequent structures for we now know that all phenomena can be calculated as successive events even when coherence reigns. For the above situation there are always reflected and transmitted beams since the momentum vector is greater within the dielectric than in air. We are in the analogy of QM *diffusion*.

Passing from the dielectric to air, we have a situation where for angles greater than a critical incident angle γ_c,

$$n\,\sin\gamma_c = 1, \tag{7}$$

total internal reflection (TIR) occurs because Snell's law cannot be satisfied. If the air region is of finite dimensions, we are in the analogy of QM *tunneling*.

The twin barrier structure, see Figure 1, is created by air zones separating two prisms from a narrow slab made of the same material as the prisms. Since the resonance phenomena that we seek to reproduce requires coherence, the total distance between the two prisms must be much smaller than the laser beam size (with one notable exception – head on incidence). For certain angles, as we shall demonstrate in the next section, transmission through the twin barriers will be unity (resonance). However, if the barriers are not of the same size resonance is attenuated. The direction normal to this twin barrier structure we call $\tilde{z}$. The overall transmission (reflection) amplitudes comprising of the entry step, twin barrier and exit step must multiply the gaussian modulation before integrating over wave number plain waves. In general this can only be done numerically. Obviously, the entry and exit step amplitudes will produce a reduction in laser intensity even at resonance. This should not be a serious problem for a steady state intensity, which can be measured over an arbitrary time interval. As a check of our results, the simpler single barrier amplitude can be derived from the twin

barrier one by setting the intermediate-slab thickness to zero. The resulting amplitude is that for a barrier width equal to the *sum* of our twin barrier sizes.

Before we calculate the transmission amplitudes, it is useful to derive the conditions for TIR. To do so we must consider two distinct cases.

• **Case (a)**. Shown in Figure 2a. From the internal triangle with angles γ, $\pi/2-\beta$, and $\pi/4$, we find

$$\gamma = \pi/4 + \beta. \tag{8}$$

TIR occurs for values $\gamma > \gamma_c$. This implies the following constraint on β

$$\sin 2\,\beta > \sin\left(2\,\gamma_c - \pi/2\right). \tag{9}$$

Observing that $\sin 2\,\beta > 0$, the previous condition is always satisfied when $\gamma_c < \pi/4$ since the right hand side is negative. Thus for $n > \sqrt{2}$ only TIR occurs. Let us now investigate the constraint on α for TIR in the case $n < \sqrt{2}$. From equation (9), we get

$$\sin 2\,\beta > 2\,\sin^2\gamma_c - 1 = \frac{2-n^2}{n^2} \;\Rightarrow\; \cos 2\,\beta < \frac{2\sqrt{n^2-1}}{n^2} \;\Rightarrow\; \sin^2\alpha > \frac{n^2-2\sqrt{n^2-1}}{2}. \tag{10}$$

Summarizing, in case (a), the conditions on the incident angle α which guarantee TIR are

$$\begin{aligned} &n > \sqrt{2}: && \forall\,\alpha, \\ &n < \sqrt{2}: \alpha > \arcsin\sqrt{\frac{n^2-2\sqrt{n^2-1}}{2}}. \end{aligned} \tag{11}$$

• **Case (b)**. Shown in Figure 2b. This is obtainable by flipping the prism (and consequently the full dielectric set up) with respect to the incoming central laser direction. Alternatively, and perhaps more practically, it is obtained from the previous case by flipping the laser beam about the normal to the prism. From the internal triangle with angles $\pi/2-\theta$, $\pi/2-\beta$, and $\pi/4$, we find

$$\gamma = \pi/4 - \beta. \tag{12}$$

TIR ($\gamma > \gamma_c$) imposes the following constraint on β

$$\sin 2\,\beta < \sin\left(\pi/2 - 2\,\gamma_c\right). \tag{13}$$

Observing that $\sin 2\,\beta > 0$, the previous condition is never satisfied if $\gamma_c > \pi/4$ since the right hand side is negative. Thus for $n < \sqrt{2}$ only diffusion occurs. For $n > \sqrt{2}$, from equation (13), we have

$$\sin 2\,\beta < 1 - 2\,\sin^2\theta_c = \frac{n^2-2}{n^2} \;\Rightarrow\; \cos 2\,\beta > \frac{2\sqrt{n^2-1}}{n^2} \;\Rightarrow\; \sin^2\alpha < \frac{n^2-2\sqrt{n^2-1}}{2}. \tag{14}$$

Finally, in case (b), the conditions on the incident angle α which guarantee TIR are

$$\begin{aligned} &n < \sqrt{2}: && \emptyset, \\ &n > \sqrt{2}: \alpha < \arcsin\sqrt{\frac{n^2-2\sqrt{n^2-1}}{2}}. \end{aligned} \tag{15}$$

4 Transmission probabilities

The principal transmission amplitude emerging from the far edge of the dielectric structure as sketched in Figure 1, is a product of three separate transition amplitudes, the entry and exit transitions and the twin barrier transition (assumed coherent in this study). Reflected amplitudes also occur at each stage and will in general give rise to secondary and higher transition amplitudes which we ignore for simplicity. Since the perpendicular momentum or wave number is of such relevance much of what follows involves the use of appropriate rotation matrices. We start with the entry step and consider, prior to convolution, an incoming plane wave.

• **Entry [air/dielectric interface]**

At this interface the standard one-dimensional step results hold with the relevant momentum given by the z_* component of $\boldsymbol{k}$. The z_* direction is normal to the interface and in terms of our original axis (chosen so that the principal direction coincides with the z-axis) it corresponds to a rotation of α around the x-axis,

$$\begin{pmatrix} z_* \\ y_* \end{pmatrix} = \begin{pmatrix} \cos\alpha & -\sin\alpha \\ \sin\alpha & \cos\alpha \end{pmatrix} \begin{pmatrix} z \\ y \end{pmatrix}.$$

The wave number components of the incoming laser beam which propagates in air can be expressed in the new axis in terms of the wave number $\boldsymbol{k}$,

$$\begin{aligned} k_{x_*} &= k_x, \\ k_{y_*} &= k_z\sin\alpha + k_y\cos\alpha = k\,\sin\alpha + k_y\cos\alpha + \mathrm{O}\left[k_x^2, k_y^2\right], \\ k_{z_*} &= k_z\cos\alpha - k_y\sin\alpha = k\,\cos\alpha - k_y\sin\alpha + \mathrm{O}\left[k_x^2, k_y^2\right]. \end{aligned} \tag{16}$$

The wave number components of the laser beam which propagates in the dielectric are

$$\begin{aligned} q_{x_*} &= k_{x_*}, \\ q_{y_*} &= k_{y_*}, \\ q_{z_*} &= \sqrt{n^2k^2 - k_{x_*}^2 - k_{y_*}^2} = n\,k\,\cos\beta - k_y\,\tan\beta\cos\alpha \\ &\quad + \mathrm{O}\left[k_x^2, k_y^2\right]. \end{aligned} \tag{17}$$

Now the expressions for the transmission (reflection) amplitudes have phases depend upon the value of z_* for the step. Our laser formulas are written with the origin as the central point of minimum transverse size of the laser beam. We denote the z_* distance of the interface from this by a_* (see Fig. 1). With these definitions, we recall the step results

$$\begin{aligned} R_{a_*}^{(1,n)} &= \frac{k_{z_*} - q_{z_*}}{k_{z_*} + q_{z_*}}\; e^{2\,i\,k_{z_*}a_*} \quad \text{and} \\ T_{a_*}^{(1,n)} &= \frac{2\,k_{z_*}}{k_{z_*} + q_{z_*}}\; e^{i(k_{z_*} - q_{z_*})a_*}. \end{aligned} \tag{18}$$

• **Exit [dielectric/air interface]**

For the exiting stage dielectric/air interface at $z_* = b_*$, we need only interchange in the entry results k_{z_*} with q_{z_*}

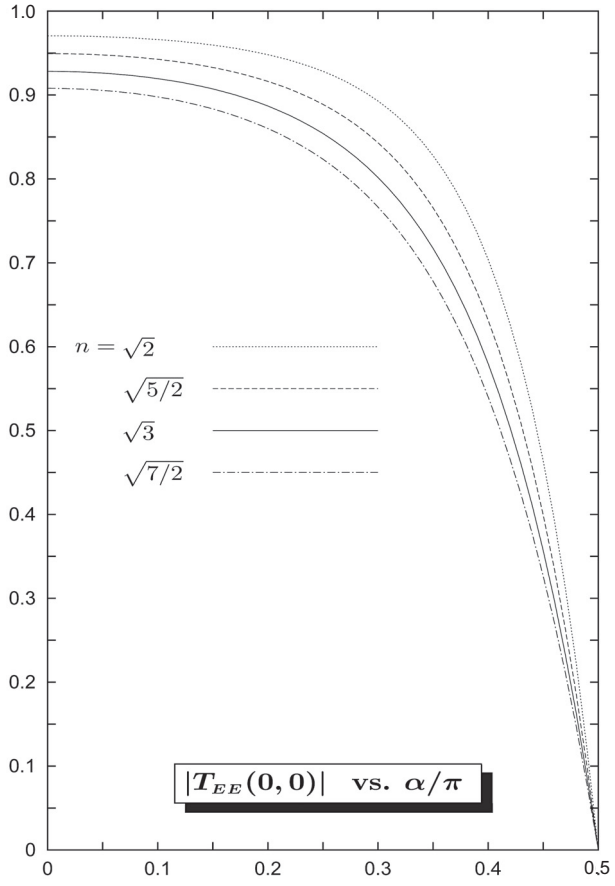

Fig. 3. The modulus of the entry exit transmission amplitude for the central (s-polarized) laser ray, $k_x = k_y = 0$, plotted as a function of the incident angle, α, for different values of refractive index, n. The continuous line corresponds to the refractive index, $n = \sqrt{3}$, used in our numerical studies. For small incidence angles, the variation is very smooth and less than 10%.

and change a_* with b_*,

$$R_{b_*}^{(n,1)} = \frac{q_{z_*} - k_{z_*}}{q_{z_*} + k_{z_*}}\ e^{2\,i\,q_{z_*} b_*} \quad \text{and}$$
$$T_{b_*}^{(n,1)} = \frac{2\,q_{z_*}}{q_{z_*} + k_{z_*}}\ e^{i(q_{z_*} - k_{z_*})b_*}. \tag{19}$$

For our calculation of the transmission amplitude, we shall need the product of the entry and exit transmission amplitudes, $T_{\rm EE}$,

$$T_{\rm EE}\,(k_x, k_y) = T_{a_*}^{(1,n)} T_{b_*}^{(n,1)} = \frac{4\,k_{z_*} q_{z_*}}{\left(k_{z_*} + q_{z_*}\right)^2}\ e^{i(q_{z_*} - k_{z_*})D_*}, \tag{20}$$

where $D_* = b_* - a_*$. In Figure 3, we show the values of the above product for different values of refractive index n as a function of the incident angle α. The values of k_x and k_y have been chosen as zero here, so these curves strictly apply to the central laser ray. The dependence is mild (particularly for small incident angles) compared, for example, to that induced by resonance (see below). Its main effect will be that of reducing the emerging laser beam intensity compared to the ingoing laser beam, even at the peak of resonance when the twin barrier amplitude is unity. As pointed out in the previous section, this should not constitute a serious problem.

• Central structure [dielectric/air/dielectric/air/ dielectric interface]

For resonance phenomena in tunnelling, we consider the central structure as small or comparable to the laser dimensions and give the overall transmission (reflection) amplitudes for this. Before doing so it is convenient to rotate the axis anew about x to define the $\tilde{z}$ direction normal to the central structure

$$\begin{pmatrix} \tilde{z} \\ \tilde{y} \end{pmatrix} = \frac{1}{\sqrt{2}} \begin{pmatrix} 1 & -1 \\ 1 & 1 \end{pmatrix} \begin{pmatrix} z_* \\ y_* \end{pmatrix}.$$

In terms of the new axis, the dielectric wave numbers become

$$\begin{aligned} q_{\tilde{x}} &= q_{x_*}, \\ q_{\tilde{y}} &= \left(q_{z_*} + q_{y_*}\right)/\sqrt{2} = n\,k\,\sin\gamma \\ &\quad + k_y\,\cos\gamma\,\cos\alpha\,/\cos\beta + \mathrm{O}\left[k_x^2, k_y^2\right], \\ q_{\tilde{z}} &= \left(q_{z_*} - q_{y_*}\right)/\sqrt{2} = n\,k\,\cos\gamma \\ &\quad - k_y\,\sin\gamma\,\cos\alpha\,/\cos\beta + \mathrm{O}\left[k_x^2, k_y^2\right], \end{aligned} \tag{21}$$

and the air wave numbers

$$\begin{aligned} k_{\tilde{x}} &= q_{\tilde{x}}. \\ k_{\tilde{y}} &= q_{\tilde{y}}, \\ k_{\tilde{z}} &= \sqrt{k^2 - q_{\tilde{x}}^2 - q_{\tilde{y}}^2} = k\,\sqrt{1 - n^2\sin^2\gamma} \\ &\quad - n\,k_y\,\frac{\sin\gamma\cos\gamma}{\sqrt{1 - n^2\sin^2\gamma}}\frac{\cos\alpha}{\cos\beta} + \mathrm{O}\left[k_x^2, k_y^2\right]. \end{aligned} \tag{22}$$

For $n\,\sin\gamma > 1$, we have tunneling. In this case, we can rewrite $k_{\tilde{z}} = i\,|k_{\tilde{z}}|$ where

$$|k_{\tilde{z}}| = k\,\sqrt{n^2\sin^2\gamma - 1} + n\,k_y\,\frac{\sin\gamma\cos\gamma}{\sqrt{n^2\sin^2\gamma - 1}}\frac{\cos\alpha}{\cos\beta} + \mathrm{O}\left[k_x^2, k_y^2\right].$$

The single barrier reflection and transmission coefficients are [17]

$$\begin{aligned} R &= -\,i\,\frac{q_{\tilde{z}}^2 + |k_{\tilde{z}}|^2}{2\,q_{\tilde{z}}\,|k_{\tilde{z}}|}\ \sinh\left(|k_{\tilde{z}}|\ \widetilde{L}\right)\ e^{i\,\varphi}\,/\,\mathcal{F} \quad \text{and} \\ T &= e^{i\left(\varphi - q_{\tilde{z}}\,\widetilde{L}\right)}\,/\,\mathcal{F}, \end{aligned} \tag{23}$$

where

$$\mathcal{F} = \sqrt{1 + \left[\frac{q_{\tilde{z}}^2 + |k_{\tilde{z}}|^2}{2\,q_{\tilde{z}}\,|k_{\tilde{z}}|}\ \sinh\left(|k_{\tilde{z}}|\ \widetilde{L}\right)\right]^2},$$
$$\varphi = \arctan\left[\frac{q_{\tilde{z}}^2 - |k_{\tilde{z}}|^2}{2\,q_{\tilde{z}}\,|k_{\tilde{z}}|}\ \tanh\left(|k_{\tilde{z}}|\ \widetilde{L}\right)\right],$$

and $\widetilde{L}$ is the dimension along the $\tilde{z}$ axis of the air gap (see the figure below). The amplitude due to a back and forth reflection within the dielectric slab region produces the following loop factor

$$R\,\exp\left[2\,i\,q_{\tilde{z}}\,\tilde{b}\right]\times R\,\exp\left[-2\,i\,q_{\tilde{z}}\,\tilde{a}\right]=$$
$$R^{2}\,\exp\left[2\,i\,q_{\tilde{z}}\left(\tilde{b}-\tilde{a}\right)\right]=-\left|R\right|^{2}\,\exp\left[2\,i\left(q_{\tilde{z}}\,\widetilde{D}+\varphi\right)\right],$$

where $\widetilde{D}$ is the dimension along the $\tilde{z}$ axis of the dielectric slab (see amplification in Fig. 1). Thus performing the sum over successive loop contributions to the twin barrier amplitude, $T_{\rm TB}$, yields

$$T_{\rm TB}\left(k_x,k_y\right)=\frac{T^{2}}{1+\left|R\right|^{2}\,\exp\left[2\,i\left(q_{\tilde{z}}\,\widetilde{D}+\varphi\right)\right]}. \qquad (24)$$

The above result can also be calculated through a standard matrix approach. A check of this result can be made by setting $\widetilde{D}=0$. This yields the single barrier result for a barrier *size* of $2\widetilde{L}$ to be compared with that for the size $\widetilde{L}$ barrier results used in the above derivation. The results are in accord.

The resonance conditions are achieved when the phase factor multiplying $\left|R\right|^{2}$ equals -1. The denominator is then equal to $\left|T\right|^{2}$ and the twin barrier amplitude reduces to a mere phase and hence of unit modulus. In general the denominator will far exceed the numerator, which for sufficiently large $\widetilde{L}$ is proportional to a decreasing exponential in $\widetilde{L}$. In Figure 4, we show some explicit examples of this phenomena. In this figure, we have set arbitrarily $k_x=0$ and $k_y=0$ and plotted $|T_{\rm TB}|$ versus the incident angle α for a refractive index $n=\sqrt{3}$. Note that this angle is not the impinging angle upon the twin barrier structure itself (see Fig. 2). The three curves are for $\{k\widetilde{L},k\widetilde{D}\}=\{1.5,100\}$, $\{1,100\}$, $\{1,500\}$. In each the resonance structure is clearly manifest. The peaks are very close to each other in the latter case. The first two plots demonstrate that for a fixed $\widetilde{D}$ the resonance peaks are narrower as $\widetilde{L}$ increases. As an aside, we recall that resonance requires the existence of a non null $\widetilde{D}$. The resonance condition cannot be obtained by φ alone. For tunnel resonance one needs multiple barriers.

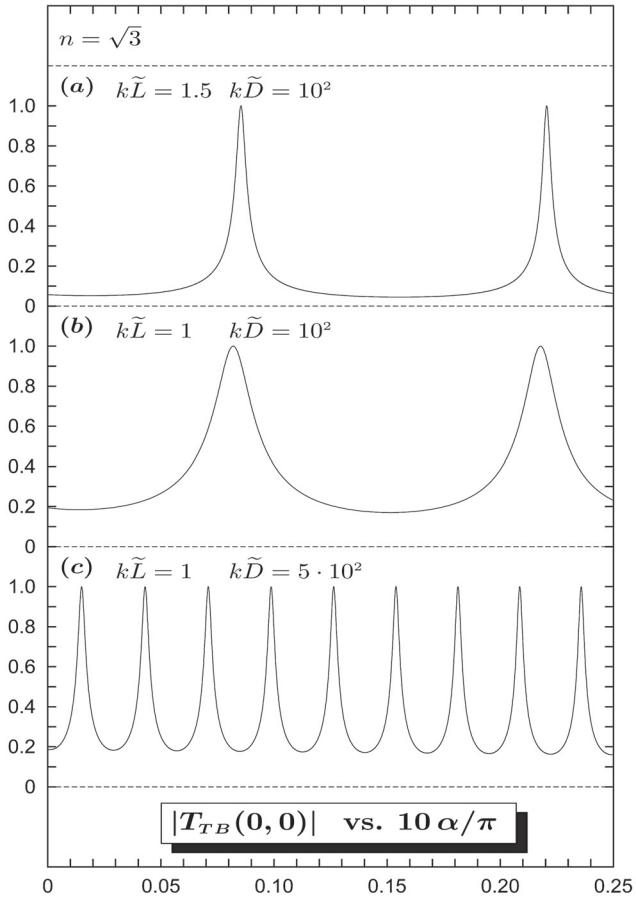

Fig. 4. The modulus of the twin barrier transmission amplitude for the central (s-poralized) laser ray, $k_x=k_y=0$, plotted as a function of the incident angle, α, for different values of the twin air gaps, $\widetilde{L}$, and the dielectric slab, $\widetilde{D}$. The resonance peaks are narrower as the air gaps increase and the distance between any two peaks decreases by increasing the dielectric slab dimension.

5 Numerical analysis

Our interest in this paper is the outgoing transmission amplitude from the twin barrier dielectric set-up described in the previous section and sketched in Figure 1. In particular, we are interested in the resonance phenomena displayed within the tunnelling regime, i.e. for TIR. TIR introduced for a step potential is somewhat of a misnomer for finite barriers. Indeed resonance, when it occurs, is the extreme counterexample since it represents *total transmission* not total reflection. The electric field for the transmitted laser is obtained by multiplying the gaussian $G(k_x,k_y)$ in equation (2) by $T_{\rm EE}(k_x,k_y)$ and $T_{\rm TB}(k_x,k_y)$,

$$E_T(x,y,z)\approx E_0\,\frac{\mathrm{w}_0^2}{4\,\pi}\int \mathrm{d}k_x\,\mathrm{d}k_y\;G\left(k_x,k_y\right)\,T_{\rm EE}\left(k_x,k_y\right)\times T_{\rm TB}\left(k_x,k_y\right)e^{i(k_x\,x+k_y\,y+k_z\,z)}.$$

Observing that $kw_0\gg1$ and that the dependence on k_x in $T_{\rm EE}\,T_{\rm TB}$ is only of second order, whereas the k_y dependence is of the first order, we can simplify the transmitted electric field as follows

$$\left|E_T(x,y,z)/E_0\right|\approx\frac{\mathrm{w}_0^2}{2\,\sqrt{\pi}\,\mathrm{w}(z)}\;\exp\left[-x^2/\mathrm{w}^2(z)\right]\times\left|\int \mathrm{d}k_y\;\;G_T\left(k_y\right)\,\exp\left[i\left(k_y\,y-\frac{k_y^2}{2k}\,z\right)\right]\right|, \qquad (25)$$

where

$$G_T\left(k_y\right)=\exp\left[-k_y^2w_0^2/4\right]\;T_{\rm EE}\left(0,k_y\right)\,T_{\rm TB}\left(0,k_y\right).$$

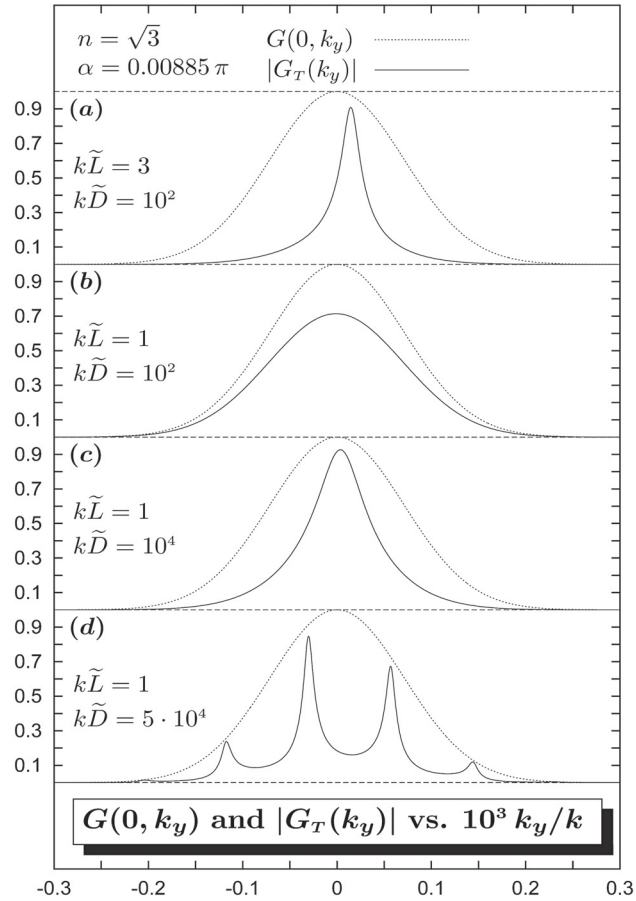

Fig. 5. The incoming gaussian distribution, $G(0, k_y)$, and the transmitted distribution, $|G_T(k_y)|$, for s-poralized laser beams of size $w_0 = 2$ mm are plotted as a function of k_y for different values of the twin air gaps, $\widetilde{L}$, and the dielectric slab, $\widetilde{D}$. The incident angle, α, is chosen around the first resonance for the first three cases, see plots (a, b, c). In the last plot (d), it is manifest the presence of multiple peaks.

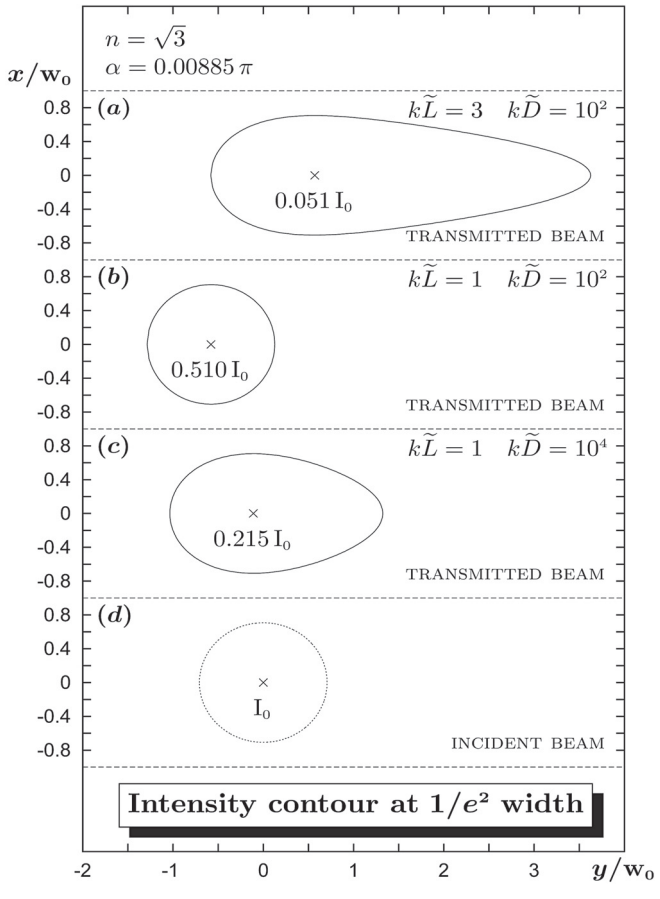

Fig. 6. The exit contour of the (s-poralized) laser intensity at $1/e^2$ width is plotted in the x-y plane for different values of the twin air gaps, $\widetilde{L}$, and the dielectric slab, $\widetilde{D}$. The distance from the source of the laser, z-axis, and the dielectric block dimension, z_*-axis, are respectively chosen to be $500w_0$ (1 m) and $50w_0$ (10 cm). The values of the peak intensities are given in terms of the incoming laser beam peak intensity I_0.

In Figure 5, we plot $|G_T(k_y)|$ as a function of k_y around the angular resonance for the following choices $\{k\widetilde{L}, k\widetilde{D}\} = \{3, 10^2\}$, $\{1, 10^2\}$, $\{1, 10^4\}$, $\{1, 5 \times 10^4\}$. Also plotted in the same figure is the incoming gaussian with $k_x = 0$, i.e. $G(0, k_y)$. The effect of $T_{\rm EE}(0, k_y)\, T_{\rm TB}(0, k_y)$ reduces the peak values of each curve and for $\{k\widetilde{L}, k\widetilde{D}\} = \{3, 10^2\}$ shifts the peak significantly to a positive value of k_y. In the case with $\{k\widetilde{L}, k\widetilde{D}\} = \{1, 5 \times 10^4\}$, we see the presence of multiple peaks. Observe that the values of $\widetilde{L}$ are very small if compared to the laser beam size, $k\widetilde{L} = 1$ corresponds to $\widetilde{L} = 0.1$ μm.

The spatial size of the laser is set by w_0 and is of 2 mm. For distances between laser source, dielectric structure and measurement apparatus of the order of a few meters we can readily neglect spatial spreading due to the gaussian, although this does not necessarily apply (as we shall see) to the effect of twin barrier resonance upon the beam. As we have argued in depth elsewhere, resonance phenomena requires a twin barrier structure smaller in size than the beam size. This means that $\widetilde{D} + 2\widetilde{L} \ll 2$ mm. Since for other reasons $\widetilde{L}$ must be much smaller (of the order of λ) this limits $\widetilde{D}$ to less than a mm. For greater values of $\widetilde{D}$ the resonance peaks proliferate so that the gaussian laser would encompass multiple resonance peaks. In this case varying the incident angle produces little or no consequences and the resonance effect is averaged out.

With the same selection of values of $\{\widetilde{L}, \widetilde{D}\}$ used in Figure 5, we have performed a numerical calculation of $|E_T(x, y, z)|^2$. In Figure 6, we plot the exit contour of the laser intensity in the x-y plane at the $1/e^2$ width. The results are, of course, correlated to those of Figure 5. For example, a narrow curve in k_y such as in Figure 5a produces a large spread in the y contour in Figure 6a. The x-spread is the same in all of the Figure 6 because the x-integral in equation (25) factorizes (after ignoring second order corrections in k_x). In Figure 6d, we display for comparison the incident laser beam with peak intensity I_0. The values of the peak intensities (all close to $x = y = 0$) are also given in each figure. Figure 5b corresponding to $\{k\widetilde{L}, k\widetilde{D}\} = \{1, 10^2\}$ is notable because it

almost reproduces the incident laser reduced in intensity by a factor of 1/2. We do not display the more complex case corresponding to Figure 5d with its multiple peaks.

6 Conclusions

We have described in this paper is some detail an optical analogy of the twin barrier resonance experiment. The presentation has been made in three dimensions for an incoming gaussian laser beam characterized by a width of $w_0 = 2$ mm. The laser wavelength has been set at $\lambda = 633$ nm and the dielectric refractive index has been arbitrarily set at $n = \sqrt{3}$. The twin barriers are reproduced by identical air intervals encompassing a narrow ($\sim$mm) dielectric slab. The width sizes which allow for a clear angular separation of resonance peaks are of the order of several μm. Concentrating upon the first resonance peak, we find a very narrow angular spread comparable to that of the laser beam itself. To clearly see the resonance peak, our primary objective in this proposal, we must have a laser spread of the order or even smaller than the resonance peak. In the contrary case, the laser beam would encompass multiple peaks and varying the incident angle α would not result in significant differences in the outgoing beam.

Once the resonance structure has been confirmed and assuming the numerical estimates of the previous sections are also convalidated, we can use the angular separation between resonance peaks to measure any of the parameters assumed in this work. For example the distance $\widetilde{D}$ or/and the barrier widths $\widetilde{L}$. The values of the resonance angles may also be used to measure the laser wavelength if all the other parameters are known. In principle, it should also be possible to detect variation in the twin nature of the barriers. This could be caused both by modifying the equal sizes of the barriers or by modifying one or both of the refractive indices of the air barriers, e.g. by density, temperature or chemical nature of the "air" enclosed. Also probable is the loss of resonance due to external disturbances such as vibrations. While these are annoying characteristics for any experiment they also open the possibility of practical applications.

The authors thank the anonymous referees for their constructive comments and useful suggestions. One of the authors (SdL) also thanks the CNPq (*Bolsa de Produtividade em Pesquisa 2010/13*) and the FAPESP (*Grant No. 10/02213-3*) for financial support.

References

1. S. De Leo, P. Rotelli, J. Opt. A Pure Appl. Opt. **10**, 115001 (2008)
2. S. De Leo, P. Rotelli, Eur. Phys. J. D **61**, 481 (2011)
3. A. Bernardini, S. De Leo, P. Rotelli, Mod. Phys. Lett. A **19**, 2717 (2004)
4. S. De Leo, P. Rotelli, Eur. Phys. J. C **46**, 551 (2006)
5. M. Born, E. Wolf, *Principles of Optics* (Cambridge UP, Cambridge, 1999)
6. G. Eichmann, J. Opt. Soc. Am **61**, 161 (1971)
7. C.K. Carniglia, L. Mandel, J. Opt. Soc. Am. **61**, 1035 (1971)
8. J.A. Arnaud, Prog. Opt. **11**, 247 (1973)
9. R.J. Black, A. Ankiewwicz, Am. J. Phys. **53**, 554 (1985)
10. J. Evans, Am. J. Phys. **61**, 347 (1993)
11. J.H. Smet et al., Phys. Rev. Lett. **77**, 2272 (1996)
12. M.A. Marte, S. Stenholm, Phys. Rev. A **56**, 2940 (1997)
13. D. Dragoman, M. Dragoman, IEEE J. Quantum Electron. **33**, 375 (1997)
14. D. Dragoman, M. Dragoman, Opt. Commun. **150**, 331 (1998)
15. D. Dragoman, Prog. Opt. **42**, 424 (2002)
16. S. Longhi, Laser Photon. Rev. **3**, 243 (2009)
17. C. Cohen-Tannoudji, B. Diu, F. Laloë, *Quantum Mechanics* (John Wiley & Sons, Paris, 1977)
18. A. Haibel, G. Nimtz, A.A. Stahlhofen, Phys. Rev. E **63**, 047601 (2001)
19. Z. Vörös, R. Johnsen, Am. J. Phys. **76**, 746 (2008)
20. S. Esposito, Phys. Rev. E **67**, 016609 (2003)
21. V.S. Olkhovsky, E. Recami, A.K. Zaichenko, Europhys. Lett. **70**, 1 (2005)
22. S. De Leo, P. Rotelli, Phys. Lett. A **342**, 294 (2005)
23. S. Hayashi, H. Kurokawa, H. Oga, Opt. Rev. **6**, 204 (1999)
24. V.S. Olkhovsky, E. Recami, J.J. Jakiel, Phys. Rep. **398**, 133 (2004)
25. S. Esposito, Phys. Rev. E **64**, 026609 (2001)
26. H.G. Winful, Phys. Rev. A **79**, 023826 (2009)